INTERNATIONAL JOURNAL OF SUSTAINABLE CONSTRUCTION ENGINEERING AND TECHNOLOGY
VOL. 14 NO. 4 (2023) 320-331

IJSCET

http://publisher.uthm.edu.my/ojs/index.php/ijscet

ISSN : 2180-3242 e-ISSN : 2600-7959

International Journal of Sustainable Construction Engineering and Technology

Geocell Reinforced Flexible Pavement: Analysis of Strain Induced in Geocell vis-a-vis Thin and Thick-walled Cylinder Theory

Shubham Prakash Shrirao[1*], Parth Rajaram Kulkarni[1], Sukhanand Sopan Bhosale[1]

[1]Department of Civil Engineering,
COEP Technological University, 411005, INDIA

[*]Corresponding Author

DOI: https://doi.org/10.30880/ijscet.2023.14.04.024
Received 18 March 2023; Accepted 18 December 2023; Available online 28 December 2023

Abstract: Vertical pressure from vehicles on pavement reinforced with geocell develops radial and hoop stresses on geocell walls. Thin-walled cylinder theory is used to estimate the strain induced in geocell by some researchers. It is observed that thin-walled cylinder theory significantly overestimates induced strain when compared with experimental values. This paper presents non-accounted effect of lateral resistance mobilized due to geocell infill soil in computing strain by thin-walled cylinder theory. It is observed that computed strain values using thin-walled cylinder theory accounting lateral resistance match well with experimental results reported in literature. Equivalent thickness (t_{eq}) of geocell is then back-calculated by matching the experimental strain values with computed strain values using thin-walled cylinder theory accounting lateral resistance. As the thickness of geocell increases in the form of $t_{eq,}$ thick-walled cylinder theory is also studied to analyze the strain induced in the geocell. Combined analysis is then carried out by modifying thick-walled cylinder theory equations using t_{eq} derived from thin-walled cylinder theory, and new factor named merging factor (M.F.) is introduced. Results of thick-walled cylinder theory with M.F. match well with experimental strain values reported in literature. Strain computed using modified thin-walled cylinder theory is validated with laboratory results of other researchers.

Keywords: Geocell, strain, thin-walled cylinder theory, thick-walled cylinder theory, equivalent thickness, merging factor

1. Introduction

In recent years, pavement construction in India has reached a record speed of 30 km per day (MORTH, 2019). Hence with evolving times, the appropriate pavement design with available construction material for cost efficiency without compromising the quality of the work to attain its required strength and durability is a stupendous task as a designer. The major failure in the flexible pavement is due to the differential settlement and bearing capacity failure of the embankment layer (Bathurst and Jarrett, 1988; Latha et al., 2001; Dash et al., 2004; Mengelt et al., 2006; Han et al., 2013; Rajagopal et al., 2014; Hegde, 2017; Mamatha and Dinesh, 2017; Shrirao and Bhosale, 2021). Above mentioned failures may be avoided by increasing the thickness of subsequent pavement layers or reinforcing base/subbase layers with geosynthetic (Giroud and Han, 2004; Tingle and Jersey, 2007; Han et al., 2010; Ingle and Bhosale, 2017; Pokharel et al., 2018;). The flexible pavement layer reinforced with geosynthetic is widely adopted because of its cost-effective and easy-to-install characteristics (Emersleben and Meyer, 2010; Hegde and Sitharam, 2014; Saride et al., 2015; Khan *et al.*, 2020). Different types of geosynthetics available in the market are geotextiles, geogrids, geonets, geocells,

*Corresponding author: sps18.civil@coep.ac.in

geofoams, etc. These geosynthetics are made of novel polymeric alloys, polyethylene, polypropylene, polyester, etc. Due to its unique 3-dimensional shape, the geocell is preferable reinforcement over soft subgrade (Kief et al., 2015; Pokharel et al., 2011; Yang et al., 2012).

Many researchers in the past have evaluated the performance of geocell by considering various aspects such as different infill materials, aspect ratio, material fabrics, surface deformation, load-carrying capacity, etc. (Biswas et al., 2013; Biswas et al., 2016; Dash et al., 2001, 2003, 2007; Mandal and Gupta, 1994, Song et al., 2018, Venkateswarlu and Hegde, 2019, Gedela and Rajagopal, 2021). Hegde and Sitharam, (2014) developed the analytical model using the thin-walled cylinder theory to predict the strain induced in the geocell by different infill materials and found an overestimation of the experimental results of instrumented geocells. Also, the same thin-walled cylinder theory is used to compute the strain induced in single, 9, and 25 geocells considering the experimental data of Emersleben and Meyer, (2010). The observed strain values using the thin-walled cylinder theory overestimated the experimental strain values of Emersleben and Meyer, (2010). Hence in this paper, the reasons for the overestimation are studied and presented.

2. Method of Analysis

Hegde and Sitharam, (2014) have neglected the influence of lateral resistance on the geocell due to the surrounding soil, which led to the overestimation of strains computed by the thin-walled cylinder theory. Hence, the lateral resistance is evaluated and there after computed strains are compared with the experimental results of Hegde and Sitharam, (2014) and Emersleben and Meyer, (2010). After accounting lateral resistance, the results match the experimental results at different lateral resistance percentages for different infill materials as well as for the different numbers of geocell. Using the strain curves obtained after accounting for lateral resistance, thickness t is back-calculated for each case using the trend line equation; this thickness is termed the equivalent thickness (t_{eq}) of the geocell. As the thickness of geocell increases in the form of $t_{eq,}$ the thick-walled cylinder theory is also studied to compute the strain induced in the geocell. However, these results are far different from experimental results.

Therefore, the combined analysis is then carried out by modifying thick-walled cylinder theory equations using t_{eq} derived from thin-walled cylinder theory. From the combined analysis, the term merging factor (M.F.) is introduced. This M.F establishes the relationship between the thin and thick-walled cylinder theories. The properties of the geocell used by several researchers during the study are given in Table 1.

Table 1 - Material Properties of Geocell

Parameter	Researchers			
	Hegde and Sitharam, (2014)	Emersleben and Meyer, (2010)	Thakur et al. (2012)	Yang et al. (2012)
Thickness, t (mm)	1.53	1.5	1.1	1.5
Equivalent Diameter, d (m)	0.258	0.258	0.29	0.28
Poisson's Ratio, μ	0.45	0.45	0.45	0.45
Modulus of Elasticity, E (MPa)	275	300	355	200
Polymer	Polyethylene	High-Density Polyethylene	Novel Polymeric Alloy	Novel Polymeric Alloy

3. Analysis of Geocell Strain Through Thin-Walled Cylinder Theory

The thin-walled cylinder theory (Shigley, 2011) is studied in many engineering applications such as pipes, LPG cylinders, storage tanks, etc., where the wall of the cylinder is subjected to internal pressure. The geocells are assessed using thin-walled cylindrical theory equations for the determination of strain-induced in the geocell wall because the thickness of the geocells is approximately 1.5 mm, which is significantly less than the diameter of the geocell and resembles the cylindrical shape. In thin-walled cylinder theory, the wall is subjected to internal stresses, and due to its inherent properties, the tensile tangential stresses are experienced by the wall of the geocell, commonly known as hoop stress, and the resultant developed strain is known as the hoop strain.

By equilibrium of forces, the equation of hoop stress is as follows:

$$\sigma_h = \frac{P \times d}{2 \times t} \quad (1)$$

Where, σ_h = Hoop Stress (kPa); P = Horizontal Pressure (kPa) = k_a x q; k_a = Coefficient of Active Pressure, q = Applied Footing Pressure (kPa); d = Diameter of Geocell (m); t = Thickness of Geocell (mm)

Hoop strain is the strain developed in the circumferential direction attributed to the radial stress distribution in geocell. The equation of hoop strain by thin-walled cylinder theory, using the principle of superposition, is as follows:

$$\varepsilon_h = \frac{P \times d}{4 \times t \times E}(2-\mu) \quad (2)$$

Where, ε_h = Hoop Strain; μ = Poisson's Ratio; E = Modulus of Elasticity (MPa)

Hegde and Sitharam, (2014) used the thin-walled cylinder theory to analyze the stresses and strain in geocells. Since the results of the strain-induced in geocell with different infill materials overestimated the experimental results of instrumented geocell, the lateral resistance is considered in the percentage of total horizontal pressure in the hoop stress equations. Thus Eq. 1 becomes

$$\sigma_h = \frac{(P - P_n) \times d}{2 \times t} \quad (3)$$

Where P_n = Percentage of Total Horizontal Pressure P

When lateral resistance is considered, the results at various resistance percentages for different infill materials are consistent with the experimental results. The t_{eq} of the geocell is determined for each case by back-calculating thickness using the strain curves obtained after taking corresponding lateral resistance into account.

Further, the strain is again computed using hoop stress and hoop strain equations by replacing thickness with a t_{eq} of geocell as follows:

$$\sigma_h = \frac{P \times d}{2 \times t_{eq}} \quad (4)$$

$$\varepsilon_h = \frac{P \times d}{4 \times t_{eq} \times E}(2-\mu) \quad (5)$$

3.1 Effect of Angle of Internal Friction (φ) on Strain

The effect of the change in φ of infill soil on the strain induced in geocell is studied with reference to the experimental results of Hegde and Sitharam, (2014). The experimental strains induced in the geocell from the study by Hegde and Sitharam, (2014) for infill soil having φ of 28°, 35°, and 40° are examined, and it is observed that the computed strains matched with the experimental strains by taking the lateral resistance into account at 10%, 25%, and 50%, respectively as shown in fig 1. Further, the experimental strains from Hegde and Sitharam's (2014) study are analyzed with the computed strains after considering t_{eq} using the thin-walled cylinder theory. The computed strains by considering t_{eq} 1.79mm, 2.28mm, and 3.15mm match well with the experimental strains of Hegde and Sitharam, (2014) for infill soil having φ of 28°, 35°and 40°, respectively. By considering the lateral resistance and the t_{eq} of the geocell, fig. 1 depicts the plotted curves for the strains induced in the geocell compared to the computed strains using the thin-walled cylinder theory.

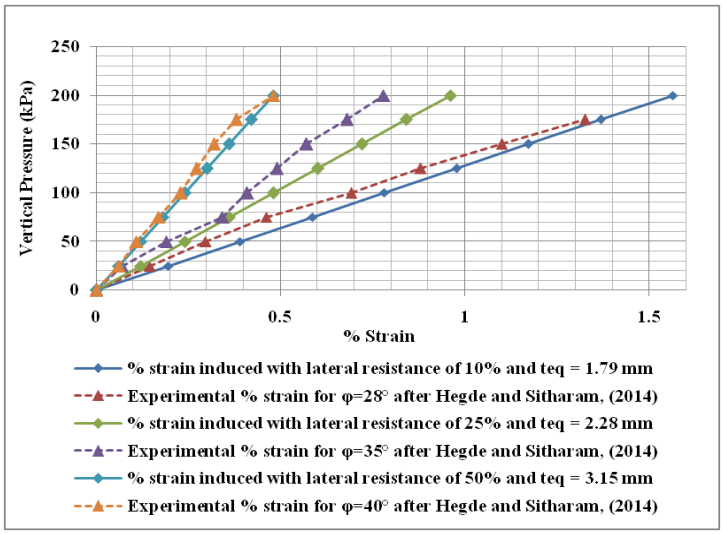

Fig. 1 - Computed values of strain-induced in geocell using thin-walled cylinder theory for infill soil of various φ by accounting percentage lateral resistance and t_{eq}

3.2 Validation of Modified Thin-walled Cylinder Theory

In accordance with the proposed equation of the thin cylinder theory for 50% lateral resistance, the average strains measured during cyclic loadings on the 15 cm and 30 cm-thick geocell-reinforced bases of Thakur et al., (2012) exhibit satisfactory agreement with a standard deviation of 0.08 and 0.1, respectively as shown in fig. 2.

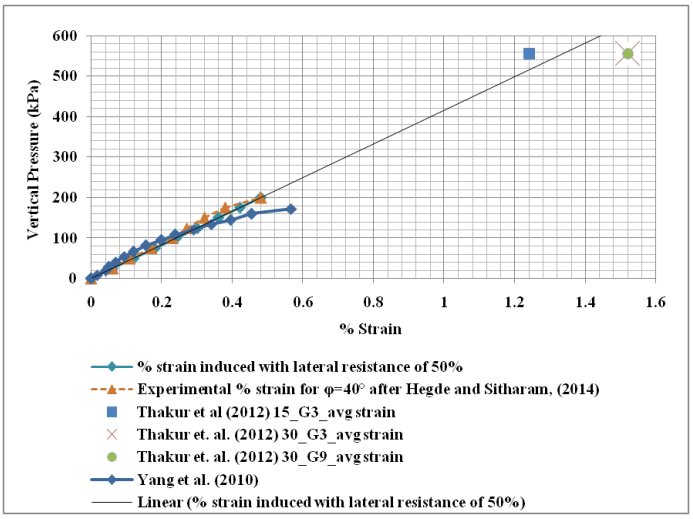

Fig. 2 - Validation of computed values of strain-induced in geocell using thin-walled cylinder theory for infill φ of 40°

Fig. 2 also shows the adequate matching of the experimental strain observed by Yang et al., (2010) with the proposed equation of thin cylinder theory for 50% lateral resistance within the standard deviation of range 0.04 to 0.11.

3.3 Effect of Number of Geocell on Strain

Emersleben and Meyer, (2010) studied the strain in geocell for single, 9, and 25 geocells infilled with the soil having a φ of 38.9°. The experimental values of the strain-induced in geocell decrease as the number of geocells increases from 1 to 25. The computed strains using lateral resistance of 10%, 25%, and 50% also match experimental strains for single, 9, and 25 geocell, respectively. It is also observed that the strains computed by considering the t_{eq} values 2.77mm, 3.57mm, and 4.34mm for 1, 9, and 25 geocell, respectively, show a satisfactory match with the variance between experimental and computed values of less than 10% (see fig. 3).

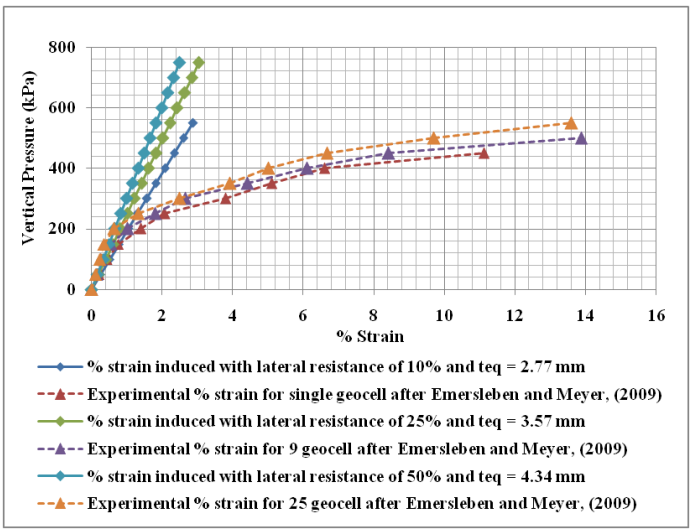

Fig. 3 - Computed values of strain-induced in geocell using thin-walled cylinder theory for single, 9, and 25 geocells

But it is observed that the computed values match only up to less than 200 kPa of applied vertical pressure, for which strain induced in geocell is 15% to 27% of failure strain (i.e., 5%) (Han et al., 2008) in geocell. After which, the

computed values are lesser and underestimate the experimental values. This might be due to linearity in the thin-walled cylinder theory equations. Also, the results depict that the increase in the number of geocells from 9 to 25 has only a marginal impact on strain induced in geocell.

4. Analysis of Geocell Strain Through Thick-Walled Cylinder Theory

The results from the thin-walled cylinder analysis show the increased t_{eq} of the geocell. Hence, the authors proposed to use a thick-walled cylinder theory (Shigley, 2011) to compute the strain induced in the geocell. During computation, the thickness of the geocell wall is assumed as the radius of the geocell, which is 125 mm. In thick-walled cylindrical theory, the prominent stresses experienced by the geocell are radial stresses and hoop stresses, which can be calculated using the following equations:

$$\sigma_r = \frac{P_i r_i^2 - P_o r_o^2}{r_o^2 - r_i^2} - \frac{r_i^2 r_o^2 (P_i - P_o)}{(r_o^2 - r_i^2) r^2} \quad (6)$$

$$\sigma_v = \frac{P_i r_i^2 - P_o r_o^2}{r_o^2 - r_i^2} \quad (7)$$

Where, σ_r = Radial Stress; σ_v = Hoop Ptress; P_i = Inner Pressure; P_0 = Outer Pressure; r_i = Inner Radius; r_0 = Outer Radius; r = Radius at which strain is calculated.

The total resultant strain experienced by the geocell is the sum of the strain induced due to hoop stress and radial stress. The equations for calculating hoop strain, radial strain, and total resultant strain are as follows:

$$\varepsilon_r = \frac{1}{E}(\sigma_r - \mu\sigma_h - \mu\sigma_v) \quad (8)$$

$$\varepsilon_h = \frac{1}{E}(\sigma_h - \mu\sigma_r - \mu\sigma_v) \quad (9)$$

$$\varepsilon = \varepsilon_h + \varepsilon_r \quad (10)$$

Where, ε_r = Radial Strain; ε_h = Hoop Strain; ε = Total Resultant Strain

The comparison of computed strains with experimental strain values of Hegde and Sitharam, (2014) and Emersleben and Meyer (2009) is depicted in fig. 4. The experimental results Hegde and Sitharam, (2014) show that strain induced in geocell decreases as the φ of soil increases. Also, Emersleben and Meyer's (2009) study illustrates the reduction in strains with an increase in the number of geocell (i.e., from 1 to 25). The computed strains by taking the geocell wall thickness as its radius are minimal, which considerably underestimate the experimental strains observed in both studies (Hegde and Sitharam, 2014; Emersleben and Meyer, 2009).

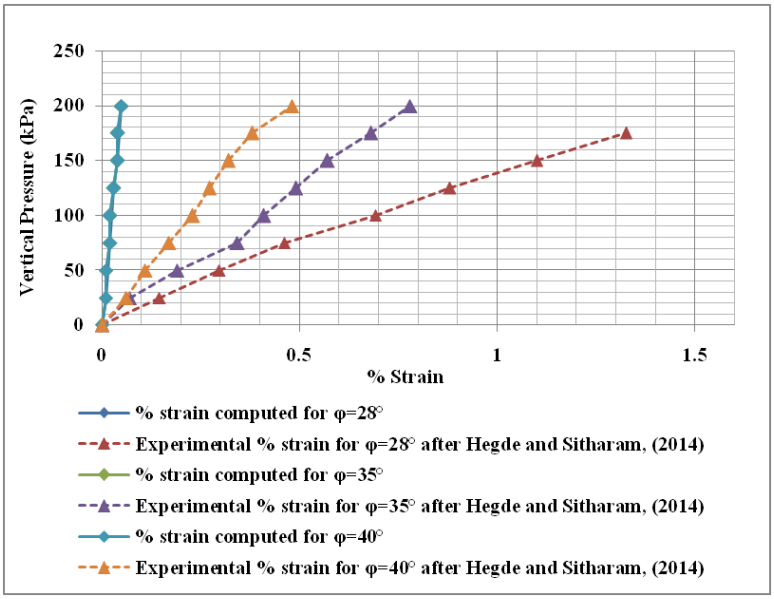

(a)

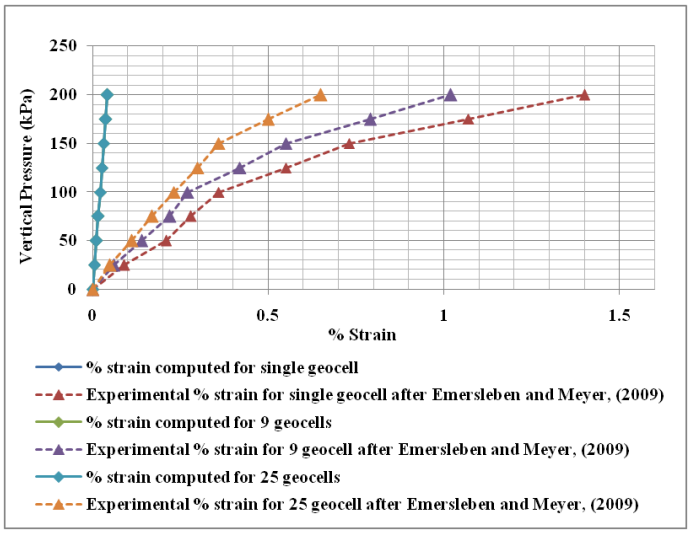

(b)

Fig. 4 - Analysis of thick-walled cylinder theory equations for the computation of strain with both (a) Hegde and Sitharam, (2014) and (b) Emersleben and Meyer, (2009)

Further, the estimated strain values decrease and undervalue the experimental strains as the thickness of the geocell wall increases with the number of adjacent cells. Hence it could be said that as the thickness of the geocell increases, the strain observed in the geocell decreases. Therefore, the thick cylinder theory cannot help to predict strain-induced in geocell under the presumptions in place. Thus the combined analysis is carried out to calculate the strains using the thick-walled cylinder theory.

Combined Analysis of Thin and Thick-walled Cylinder Theory

The combined analysis is performed by equating the strains obtained from thin-walled cylinder theory considering t_{eq}, with the total resultant strains obtained from thick-walled cylinder theory to compute the net horizontal stress on the geocell wall. The thick cylinder theory equations are solved to derive the net horizontal pressure equation by keeping the pressure and radius values unknown. The equation of net horizontal pressure is as follows:

$$2P_o r_o^2 - 1.1\ P_i r_o^2 - 0.9\ P_i r_i^2 = \varepsilon \times E \qquad (11)$$

The combined analysis results are plotted in Fig. 5, the values of strain induced in geocell by thin cylinder theory are plotted against the applied vertical pressure on the x and y-axis, respectively. Further, the computed values of net horizontal pressure from eq. 11 are plotted on the secondary y-axis. The merging factor is determined for infill soil with a φ of 28°, 35°and 40° and also, to the varying number of geocells, i.e., single, 9, and 25 geocell. The combined analysis results depict that as the φ of infill soil increases, the M.F. increases, whereas M.F. decreases marginally as the number of geocells increases. The combined analysis is summarized in Table 2.

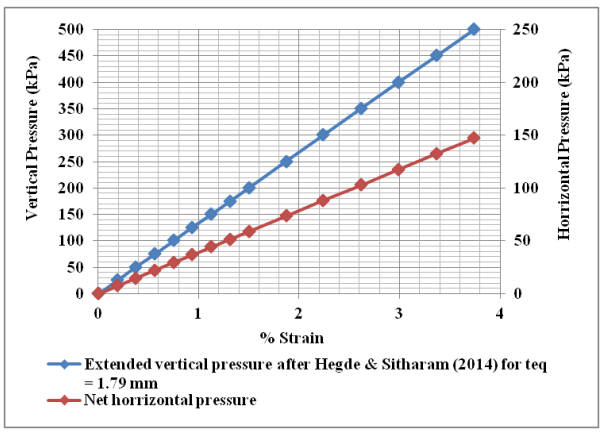

(a)

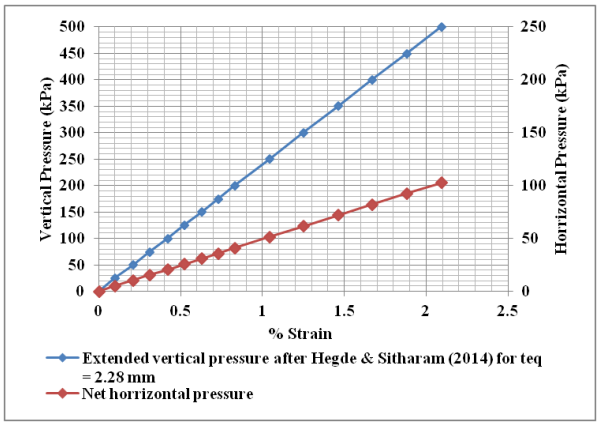
Vertical Pressure (kPa)
Horizontal Pressure (kPa)
% Strain
Extended vertical pressure after Hegde & Sitharam (2014) for teq = 2.28 mm
Net horrizontal pressure

(b)

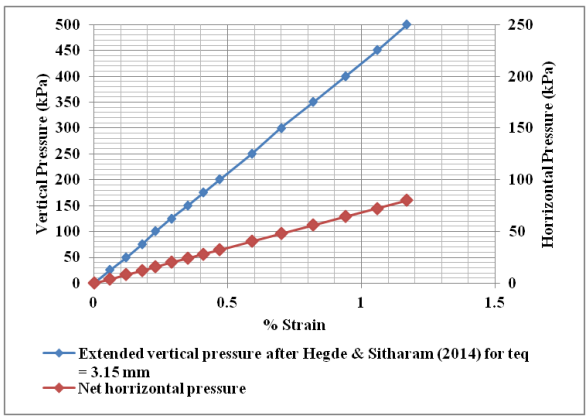
Vertical Pressure (kPa)
Horizontal Pressure (kPa)
% Strain
Extended vertical pressure after Hegde & Sitharam (2014) for teq = 3.15 mm
Net horrizontal pressure

(c)

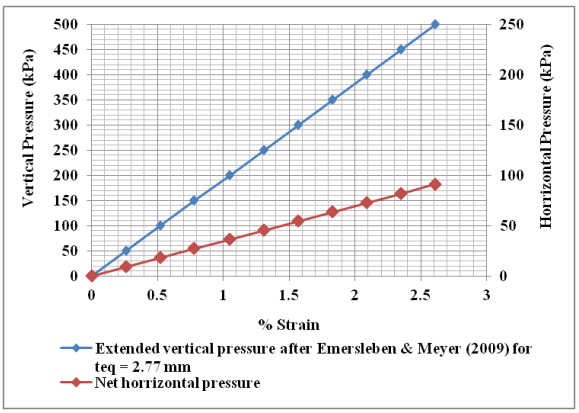
Vertical Pressure (kPa)
Horizontal Pressure (kPa)
% Strain
Extended vertical pressure after Emersleben & Meyer (2009) for teq = 2.77 mm
Net horrizontal pressure

(d)

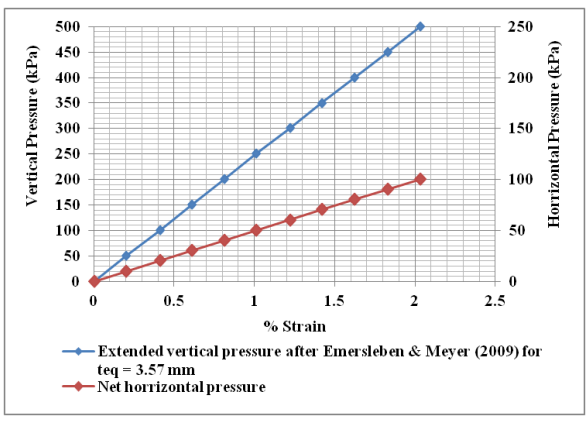
Vertical Pressure (kPa)
Horizontal Pressure (kPa)
% Strain
Extended vertical pressure after Emersleben & Meyer (2009) for teq = 3.57 mm
Net horrizontal pressure

(e)

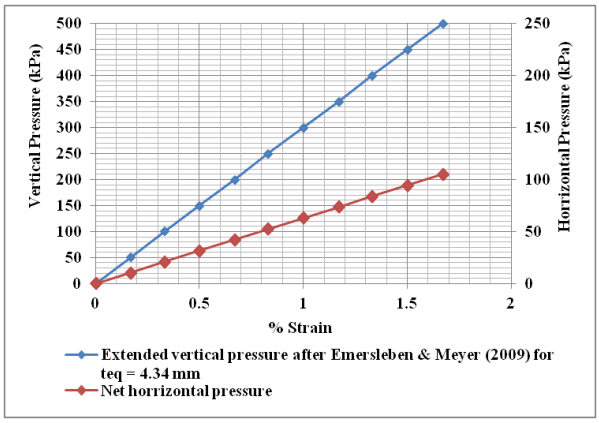

(f)

Fig. 5 - Combined analysis of thin thick-walled cylinder theories for infill soil having φ = 28° (a), 35° (b), 40° (c), and single (d), 9 (e) and 25 (f) geocells

Table 2 - Summary of Combined Analysis

Parameters	Researchers					
	(Hegde and Sitharam, 2014)			(Emersleben and Meyer, 2010)		
φ of infill soil	28°	35°	40°	38.9°		
Number of geocells	1	1	1	1	9	25
% Lateral Resistance	10 %	25 %	50 %	10 %	25 %	50 %
t_{eq}	1.79 mm	2.28 mm	3.15 mm	2.77 mm	3.57 mm	4.34 mm
t_{eq} /tactual	1.19	1.52	2.03	1.63	2.1	2.55
M.F.	3.42	4.83	6.24	5.47	4.98	4.76
Estimated compared to failure strain	26.8 %	24.16 %	15.84 %	20.13 %	16.64 %	15.78 %

The M.F derives the relationship between the thin-walled cylinder theory and the thick-walled cylinder theory. Also, it is observed that the M.F. depends upon the φ of infill soil rather than the number of surrounding geocell. Fig. 6 established the relation between the φ of infill soil and M.F. The results in fig. 6 indicate a decrease in M.F. with the reduction in the φ of infill soil. The φ at which the M.F. of the infill soil is zero is predicted with an extended trend line at 13.20°, beyond which the M.F. tends to be negative, which has no practical relevance. Also, the graph of the non-dimensional thickness parameter (t_{eq}/t_{actual}) against the φ of infill soil for a single geocell is plotted in fig. 7. The results show that as the φ of infill soil increases, the non-dimensional thickness parameter also increases. Hence, the φ of infill soil in the geocell significantly impacts the lateral resistance experienced by the geocell subjected to loading.

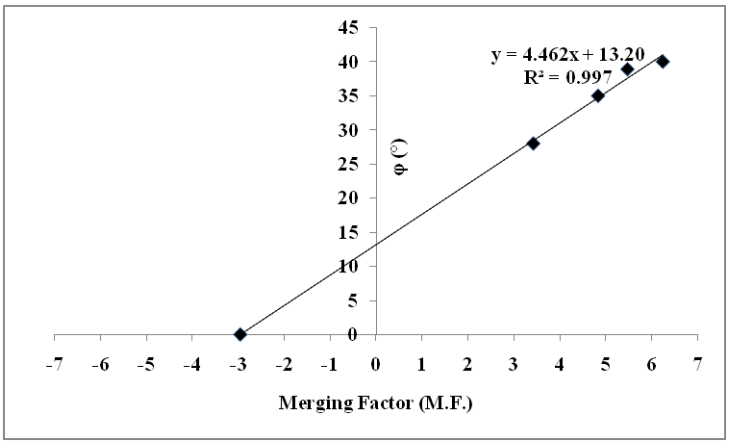

Fig. 6 - Effect of φ of infill soil on M.F.

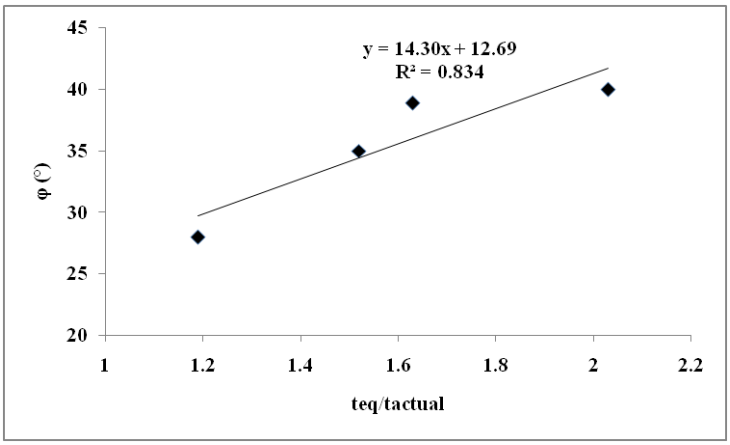

Fig. 7 - Effect of φ of infill soil on non-dimensional thickness parameter

Fig. 8 shows the effect of the number of geocells on the M.F. The results depict that the M.F. curve becomes asymptotic after 9 geocells; hence it can be said that the geocell beyond two surrounding layers may have a marginal contribution to the lateral resistance developed.

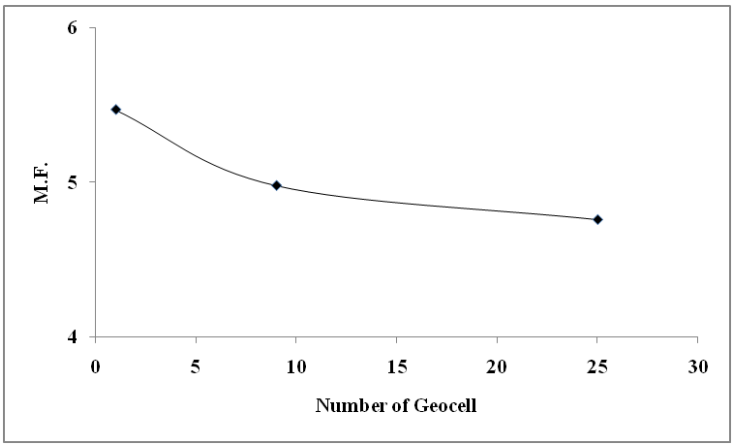

Fig. 8 - Effect of the number of geocells on the M.F.

5. Concluding Remarks

This paper presented the thin as well as thick-walled cylinder theory to estimate the strain in geocell for different infill materials. Based on the study following conclusions are drawn.

1. The overestimation of strain induced in geocell by thin-walled cylinder theory compared to the experimental results of (Hegde and Sitharam, 2014) is attributed to the non-account of lateral resistance offered by the surrounding soil.
2. The computed strain in a geocell of teq by the thin-walled cylinder theory matches well with the experimental results of Hegde and Sitharam, (2014), while for Emersleben and Meyer, (2010), the computed strains satisfactory match up to 16 to 29 % of the failure strains in the geocell.
3. To validate the thin-walled cylinder theory, the authors compare the experimental strain values of Thakur et al., (2012) and Yang et al., (2008) with the computed strains using thin-walled cylinder theory equations for 50 % lateral resistance. Here it is found that the average strains measured during cyclic loadings on the 15 cm and 30 cm-thick geocell-reinforced bases of Thakur et al., (2012) exhibit satisfactory agreement with a standard deviation of 0.08 and 0.1, respectively. Also, the experimental strains recorded by Yang et al., (2010) correspond well with the computed strains within the standard deviation of range 0.04 to 0.11.
4. The teq is directly proportional to the φ of infill soil and the surrounding number of geocell.
5. The thick-walled cylinder theory is also studied for the increased in the thickness of geocell in the form of teq. However, the strains computed by the thick-walled cylinder theory for single or multi-geocell do not match the experimental strains. The M.F. is then introduced from combined analysis to establish the relation between thin and thick-walled cylinder theories.
6. For practical relevance, the M.F. will be applicable for soil having $\varphi > 13.20°$.
7. The geocell beyond two adjacent layers might have made a small contribution to the lateral resistance formed. Therefore, the M.F. is barely influenced by geocell when it extends beyond two adjacent layers. As a result, the M.F. only depends on the infill soil.

Author Contributions

Conceptualization, S.P.S., P.R.K. and S.S.B.; methodology, S.P.S., P.R.K. and S.S.B.; validation, S.P.S. and P.R.K.; formal analysis, S.P.S. and P.R.K.; investigation, S.P.S., P.R.K. and S.S.B.; writing-draft preparation, S.P.S., P.R.K. and S.S.B.; supervision, S.S.B.; project administration, S.S.B; writing-final manuscript preparation, S.P.S. and S.S.B.;. All authors read and edited the paper before submission.

Acknowledgement

The authors gratefully acknowledge the support given by COEP Technological University, Pune and AICTE (NDF Scheme) required during completion of this work.

Notations

t_{eq}	Equivalent Thickness (mm)
M.F.	Merging Factor
φ	Angle of Internal Friction (º)
σ_h	Hoop Stress (kPa)
P	Horizontal Pressure (kPa)
k_a	Coefficient of active Pressure
q	Applied footing Pressure (kPa)
d	Diameter of Geocell (m)
t	Thickness of Geocell (mm)
μ	Poisson's Ratio
E	Modulus of Elasticity (MPa)
P_n	Percentage of Total Horizontal Pressure P
σ_r	Radial Stress (kPa)
σ_h	Hoop Stress (kPa)
P_i	Inner Pressure (kPa)
P_0	Outer Pressure (kPa)
r_i	Inner Radius (m)
r_0	Outer Radius (m)
r	Radius at which strain is calculated (m)
ε_r	Radial Strain (%)
ε_h	Hoop Strain (%)
ε	Total Resultant Strain (%)

References

Bathurst, R.J., Jarrett, P.M., 1988. Large-scale model tests of geocomposite mattresses over peat subgrades. *National Research Council, Transportation Research Board.* http://onlinepubs.trb.org/Onlinepubs/trr/1988/1188/1188-003.pdf

Biswas, A., Krishna, A. M., Dash, S.K., 2013. Influence of subgrade strength on the performance of geocell-reinforced foundation systems. *Geosynthetics International,* 20(6), 376–388. https://doi.org/10.1680/gein.13.00025

Biswas, A., Krishna, A.M., Dash, S.K., 2016. Behaviour of geosynthetic reinforced soil foundation systems supported on stiff clay subgrade. *International Journal of Geomechanics,* 16(5), 1–15. https://doi.org/10.1061/(ASCE)GM.1943-5622.0000559

Dash, S.K., Krishnaswamy, N.R., Rajagopal, K., 2001. Bearing capacity of strip footings supported on geocell reinforced sand. *Geotextiles and Geomembranes,* 19(4), 235–256. https://www.academia.edu/10304962/Mekanika_Tanah

Dash, S.K., Rajagopal, K., Krishnaswamy, N.R., 2004. Performance of different geosynthetic reinforcement materials in sand foundations. *Geosynthetics International,* 11(1), 35–42. https://doi.org/10.1680/gein.2004.11.1.35

Dash, S.K., Rajagopal, K., Krishnaswamy, N.R., 2007. Behaviour of geocell-reinforced sand beds under strip loading. *Canadian Geotechnical Journal,* 44(7), 905–916. https://doi.org/10.1139/T07-035

Dash, S.K., Sireesh, S., Sitharam, T.G., 2003. Model studies on circular footing supported on geocell reinforced sand underlain by soft clay. *Geotextiles and Geomembranes,* 21(4), 197–219. . https://doi.org/10.1016/S0266-1144(03)00017-7

Emersleben, A., Meyer, M., 2010. The influence of hoop stresses and earth resistance on the reinforcement mechanism of single and multiple geocells. 9*th International Conference on Geosynthetics - Geosynthetics: Advanced Solutions for a Challenging World, ICG 2010,* 713–716.

Gedela, R., Karpurapu, R., 2021. Influence of pocket shape on numerical response of geocell reinforced foundation systems. *Geosynthetics International,* 28(3), 327-337. https://doi.org/10.1680/jgein.20.00042

Giroud, J.P., Han, J., 2004. Design Method for Geogrid-Reinforced Unpaved Roads. I. Development of Design Method. *Journal of Geotechnical and Geoenvironmental Engineering,* 130(8), 775–786. https://doi.org/10.1061/(ASCE)1090-0241(2004)130:8(775)

Han, J., Pokharel, S.K., Yang, X., Manandhar, C., 2011. Performance of geocell-reinforced RAP bases over weak subgrade under full-scale moving wheel loads. *Journal of Materials in Civil Engineering,* 1525. https://doi.org/10.1061/(ASCE)MT.1943-5533.0000286

Han, J., Thakur, J.K., Parsons, R.L., Pokharel, S.K., Leshchinsky, D., Yang, X., 2013. A summary of research on geocell-reinforced base courses. *Proceedings of Design and Practice of Geosynthetic-Reinforced Soil Structures, eds. Ling H, Gottardi G, Cazzuffi D, Han J and Tatsuoka F, Bologna, Italy,* 351-358. doi: 10.13140/RG.2.1.4185.7129

Han J, Yang X, Leshchinsky D, Parsons RL (2008) Behavior of Geocell-Reinforced Sand under a Vertical Load. *Transportation Research Record, Journal of Transportation Research Board* 2045:95–101. https://doi.org/10.3141/2045-11

Hegde, A., 2017. Geocell reinforced foundation beds-past findings, present trends and future prospects: A state-of-the-art review. *Construction and Building Materials,* 154, 658–674. https://doi.org/10.1016/j.conbuildmat.2017.07.230

Hegde, A., Sitharam, T.G., 2014. Joint Strength and Wall Deformation Characteristics of a Single-Cell Geocell Subjected to Uniaxial Compression. *International Journal of Geomechanics,* 15(5), 04014080. https://doi.org/10.1061/(asce)gm.1943-5622.0000433

Ingle, G.S., Bhosale, S.S., 2017. Full-scale laboratory accelerated test on geotextile reinforced unpaved road. *International Journal of Geosynthetics and Ground Engineering,* 3(4),1-11. doi:10.1007/s40891-017-0110-x

Khan, M.A., Biswas, N., Banerjee, A., Puppala, A.J., 2020. Field performance of geocell reinforced recycled asphalt pavement base layer. *Transportation Research Record,* 2674(3), 69-80. https://doi.org/10.1177/0361198120908861

Kief, O., Schary, Y., Pokharel, S.K., 2015. High-Modulus Geocells for Sustainable Highway Infrastructure. *Indian Geotechnical Journal,* 45(4), 389–400. https://doi.org/10.1007/s40098-014-0129-z

Latha, G.M., Rajagopal, K., Krishnaswamy, N.R., 2001. Measurement of strains in geocells supporting an embankment. *Geosynthetics Conference* 2001.

Mamatha, K.H., Dinesh, S.V., 2017. Performance evaluation of geocell-reinforced pavements. *International Journal of Geotechnical Engineering,* 6362(July). 1–10. https://doi.org/10.1080/19386362.2017.1343988

Mandal, J. N., Gupta, P. 1994. Stability of geocell-reinforced soil', *Construction and Building Materials,* 8(1), 55–62. https://doi.org/10.1016/0950-0618(94)90009-4

Mengelt, M., Edil, T.B., Benson, C.H., 2006. Resilient modulus and plastic deformation of soil confined in a geocell. *Geosynthetics International,* 13(5). https://doi.org/10.1680/gein.2006.13.5.195

MORTH., 2019. Government of India Ministry of Road Transport & Highways New Delhi. 1–107. :https://morth.nic.in

Pokharel, S.K., Han, J., Manandhar, C., Yang, X., Leshchinsky, D., Halahmi, I., Parsons, R.L., 2011. Accelerated pavement testing of geocell-reinforced unpaved roads over weak subgrade. *Transportation research record*, 2204(1), 67-75. https://doi.org/10.1016/j.ijprt.2017.03.007

Pokharel, S.K., Han, J., Leshchinsky, D., Parsons, R.L., 2018. Experimental evaluation of geocell-reinforced bases under repeated loading. *International Journal of Pavement Research and Technology*, 11(2), 114-127. https://doi.org/10.3141/2204-09

Rajagopal, K., Chandramouli, S., Parayil, A., Iniyan, K., 2014. Studies on geosynthetic-reinforced road pavement structures. *International Journal of Geotechnical Engineering*, 8(3), 287-298. https://doi.org/10.1179/1939787914Y.0000000042

Saride, S., Rayabharapu, V.K., Vedpathak, S., 2015. Evaluation of rutting behaviour of geocell reinforced sand subgrades under repeated loading. *Indian Geotechnical Journal*, 45(4), 378-388. https://doi.org/10.1007/s40098-014-0120-8

Shigley, J.E., 2011. Shigley's mechanical engineering design. Tata McGraw-Hill Education.

Shrirao, S.P., Bhosale, S.S., 2021. Geocell Reinforced Soil/Subgrade: Comparative Study of Bearing Capacity Evaluation Methods. *Journal of University of Shanghai for Science and Technology*, 23(6), 595–605.

Song, F., Liu, H., Hu, H., Xie, Y., 2018. Centrifuge tests of geocell-reinforced retaining walls at limit equilibrium. *Journal of Geotechnical and Geoenvironmental Engineering*, 144(3), 04018005. . https://doi.org/10.1061/(ASCE)GT.1943-5606.0001849

Thakur, J.K., Han, J., Pokharel, S.K., Parsons, R.L., 2012. Performance of geocell-reinforced recycled asphalt pavement (RAP) bases over weak subgrade under cyclic plate loading. *Geotextiles and Geomembranes*, 35, 14-24. https://doi.org/10.1016/j.geotexmem.2012.06.004

Tingle, J.S., Jersey, S.R., 2007. Empirical design methods for geosynthetic-reinforced low-volume roads. *Transportation Research Record*, 2(1989), 91–101. https://doi.org/10.3141/1989-52

Venkateswarlu, H., Hegde, A., 2020. Effect of infill materials on vibration isolation efficacy of geocell-reinforced soil beds. *Canadian Geotechnical Journal*, 57(9), 1304-1319. https://doi.org/10.1139/cgj-2019-0135

Yang, X., Han, J., Pokharel, S.K., Manandhar, C., Parsons, R.L., Leshchinsky, D., Halahmi, I., 2012. Accelerated pavement testing of unpaved roads with geocell-reinforced sand bases. *Geotextiles and Geomembranes*, 32, 95-103. https://doi.org/10.1016/j.geotexmem.2011.10.004